Binary and Recoil Collisions in Strong Field Double Ionization of Helium

A. Staudte,[1,*] C. Ruiz,[2] M. Schöffler,[3] S. Schössler,[3] D. Zeidler,[4] Th. Weber,[5] M. Meckel,[3] D. M. Villeneuve,[1] P. B. Corkum,[1] A. Becker,[2] and R. Dörner[3]

[1]*National Research Council, 100 Sussex Drive, Ottawa, Ontario K1A 0R6, Canada*
[2]*Max-Planck-Institut für Physik komplexer Systeme, Nöthnitzer Strasse 38, 01187 Dresden, Germany*
[3]*Institut für Kernphysik, J. W. Goethe Universität Frankfurt, Max-von-Laue-Strasse 1, 60438 Frankfurt, Germany*
[4]*Carl Zeiss SMT AG, Rudolf-Eber-Strasse 2, 73447 Oberkochen, Germany*
[5]*Lawrence Berkeley National Laboratory, Berkeley, California 94720, USA*

(Received 14 May 2007; published 28 December 2007)

We have investigated the correlated momentum distribution of both electrons from nonsequential double ionization of helium in a 800 nm, 4.5×10^{14} W/cm^2 laser field. Using very high resolution coincidence techniques, we find a so-far unobserved fingerlike structure in the correlated electron momentum distribution. The structure can be interpreted as a signature of the microscopic dynamics in the recollision process. We identify features corresponding to the binary and recoil lobe in field-free $(e, 2e)$ collisions. This interpretation is supported by analyzing *ab initio* solutions of a fully correlated three-dimensional helium model.

DOI: 10.1103/PhysRevLett.99.263002 PACS numbers: 32.80.Rm, 31.90.+s, 32.80.Fb, 32.80.Wr

Today, it is well established that for infrared wavelengths at intermediate intensities (10^{13}–10^{15} W/cm^2) the emission of more than one electron from an atom or molecule proceeds via the rescattering mechanism [1]. According to this picture, first one electron is excited by the field to the continuum, it is then accelerated and driven back to its parent ion by the oscillating field where it can supply energy to liberate a second or even more electrons. The last step of the mechanism can be considered as an internal laser assisted electron-impact ionization of the residual ion. From the field-free counterpart (e.g., [2,3]), it is well known that after an electron-electron encounter the electrons either leave the ionic potential without further interaction (binary collision) or the incident electron gets additionally backreflected by the ion (recoil collision).

The observation of the correlated momenta (k_a, k_b) of both electrons (a, b) has been shown to provide a solid basis for an analysis of the rescattering dynamics. In many experiments [4–9] a maximum was observed for the emission of both electrons in the same direction with similar momentum components parallel to the laser field ($k_a^{\parallel} = k_b^{\parallel}$). This seemingly well established maximum is supported by numerous theoretical results (e.g., [10–12]) but is in conflict with others [13–17] which predict a minimum.

We have performed a new high resolution and high statistics experiment on double ionization of helium. Unlike previous experimental work our enhanced resolution and statistics unveil a minimum along $k_a^{\parallel} = k_b^{\parallel}$ bearing strong resemblance to the theoretical work in [15]. Our experimental observations are qualitatively reproduced by results of calculations using a recently introduced fully correlated two-electron quantum model [18]. Analysis of the temporal evolution of the momentum distributions in the *ab initio* calculations as well as simple classical estimations let us interpret the basic features of the momentum distribution in view of binary and recoil collisions.

Our experiment was performed using cold target recoil ion momentum spectroscopy (COLTRIMS) [19,20]. Ti:sapphire laser pulses (40 fs, 800 nm, 5 μJ, 100 kHz repetition rate) are focused to peak intensity of $(4.5 \pm 0.5) \times 10^{14}$ W/cm^2 into a supersonic ^{4}He gas jet. The peak intensity in the laser pulse was determined by calibrating the pulse energy-to-intensity relation using the radial ion and electron momentum in a separate experiment in circularly polarized laser pulses [21]. The result was verified by fitting the predictions of tunnel theory [22] to the He^+ momentum distribution parallel to the laser field.

Ions and electrons created in the focus are guided by a 1.6 V/cm electric and a 10.5 G magnetic field towards two large area microchannel plate detectors (Ø 80 mm) with delay line position encoding [23]. The polarization axis of the laser is parallel to the spectrometer field. In the following we present only the momenta along the polarization, i.e., momenta measured via the time of flight of ions and electrons. We detect the ion and one electron, and for a fraction of phase space of double ionization we also detect both electrons. We find a resolution (FWHM) of <0.08 a.u. parallel and <0.14 a.u. perpendicular to the laser polarization axis. To avoid any problems with the dead time of the electron detector, we generally calculate the second electron from the measured electron and ion momentum using momentum conservation.

We use a laser repetition rate of 100 kHz. This yielded a count rate of ≈ 3 kHz on the ion detector and ≈ 10 kHz on the electron detector including stray electrons and dark counts. The fraction of false coincidences, where the detected ion and electron originate from two different atoms ionized in the same laser pulse, was monitored in the single

ionization channel (compare Fig. 1 in [4]). We find that 7% of electrons and ions do not obey momentum conservation, i.e., are not from the same atom. The base vacuum in our chamber was about 10^{-10} mbar. The remaining background of H_2^+ ions from the residual gas can be very efficiently suppressed by our three-dimensional momentum imaging. He^{2+} ions have a very narrow momentum distribution perpendicular to the polarization (0.8 a.u. FWHM). The H_2^+ ions from the residual gas in contrast have a thermal momentum distribution ($\approx$5 a.u. FWHM). Therefore, selecting transverse He^+ momenta $<$0.8 a.u. efficiently suppresses the H_2^+ background. Cold H_2 contamination in the gas jet has been frozen out by cooling our nozzle on a cryogenic cold head to $\approx$14 K. A small remaining contribution is still visible in Fig. 1(a). Its position off the diagonal reflects the nuclear mass defect in helium. A total of 10^9 events contained 10^5 valid coincidences of a He^{2+} and at least one electron.

Figure 1(a) shows the final momentum correlation of the two electrons along the polarization axis. Since both electrons are indistinguishable, the data were symmetrized by exchanging the two electron indices. The first and third quadrants thus correspond to events where both electrons

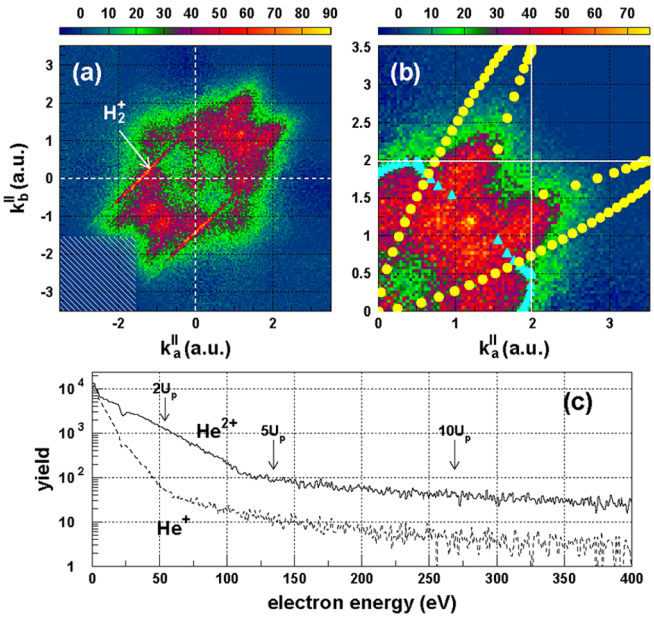

FIG. 1 (color online). (a) Correlated electron momenta for double ionization of helium at 800 nm, 4.5×10^{14} W/cm^2. Shown are the momentum components $k_{a,b}^{\parallel}$ along the polarization direction. Quadrants 1 and 3 correspond to both electrons traveling into the same hemisphere. The indicated lines are H_2^+ background from cold H_2 in our gas jet. All other background has been subtracted. (Hatched area) Detection limit for $k_{a,b}^{\parallel}$ away from the electron detector. (b) Same as (a), only 1st quadrant is shown, superimposed are the results of a classical $(e, 2e)$ scattering model (see text for details). (Solid lines) $2\sqrt{U_p}$ cutoff momentum for tunneled electrons. (c) Electron energy spectrum of He^{2+} and He^+ (normalized to He^{2+}).

are detected in the same hemisphere, while the second and fourth quadrants relate to final electron momenta that are pointing back-to-back. We find a striking fingerlike structure producing a minimum along the diagonal of equal momenta.

What is the origin of the fingerlike structure? At first glance one realizes that the structure extends beyond the limit of $2\sqrt{U_p}$ [white solid lines in Fig. 1(b)], which is the classical limit expected for a joint emission of both electrons upon a binary collision at the zero of the field. Here $U_p = I/4\omega^2$ is the ponderomotive potential determined by the intensity I and frequency ω of the field (atomic units are used throughout this Letter unless otherwise indicated). This enhancement in the production of hot electrons compared to an uncorrelated model becomes even more striking in Fig. 1(c). Here, the electron energy spectrum of He^{2+} is compared to the single ionization channel. Only electrons emitted towards the electron detector ($k^{\parallel} \geq 0$) are included. Hence, we anticipate that an electron with final momentum beyond the classical limit has interacted with the nucleus. Such a process is well known in field-free $(e, 2e)$ processes as recoil collision. To gain insight, we have determined the kinematical constraints in correlated momentum space for various $(e, 2e)$ scenarios using a simple classical model.

Our classical one-dimensional model neglects the parent ion potential as well as the long-range electron-electron repulsion. In the scenario of a binary collision, the momentum direction of the recolliding electron is unchanged. For a recoil collision, the direction of the momentum of the first electron is inverted (i.e., the electron is scattered by 180°). In both scenarios the impact energy of the recolliding electron is reduced by the binding energy and the second electron is born with zero momentum.

In Fig. 1(b) we have superimposed the kinematical constraints obtained from the classical model for the binary collision (circles) and for the recoil collision (triangles) with the experimental data of the first quadrant. The comparison reveals a strong correspondence between the features seen in the experimental data and the classical estimations. The binary collision scenario leads to a broad distribution. But more interestingly, the estimations based on a recoil collision exhibit the prominent fingerlike structure beyond the limit of $2\sqrt{U_p}$.

The assumed asymmetric energy sharing of the excess electron-impact energy is typical in field-free $(e, 2e)$ processes [24]. It also yields the best correspondence with the experimental data compared to a more symmetric energy sharing. Classical estimates including excited states of the He^+ ion have shown that recollision excitation with subsequent tunneling ionization (RESI) [5] is not responsible for the fingerlike structure.

Next, we show that the results of our classical analysis are supported by quantum mechanical calculations. To this end, we have performed *ab initio* numerical simulations

using a recently introduced helium model [18], in which the center-of-mass motion of the two electrons is restricted to the polarization axis, while the electron correlation is fully retained via the relative coordinate of the electrons.

In our simulation the coupling to the laser field is done using the velocity gauge and within the dipole approximation. We have used an artificial laser pulse with a linear ramp over two cycles to the peak intensity of 5×10^{14} W/cm^2 at 800 nm where it was kept constant for two more oscillations of the field [see Fig. 2(a)]. The initial wave function has been obtained via imaginary time propagation and has been propagated using the Crank-Nicholson method on a grid with $3000 \times 1500 \times 400$ points, other grid parameters were as in [18].

In the simulation a restriction to a few oscillations of the laser field is necessary in order to keep the full wave function on the grid for a determination of the momentum distribution at the end of the calculation. This requires a large amount of computer resources (in time as well as in memory), which quickly grows with the number of cycles of the pulse. In fact, the proposed mechanism requires the analysis of only a single rescattering event shortly after the impact, without the obscuring contributions from earlier rescattering events. The latter is achieved by the fast turn on of the field.

In Fig. 2 we show the distribution of the correlated two-electron momentum components along the polarization direction at some time during the pulse [2(b)] and at the end of the pulse [2(c)]. The distributions are obtained by

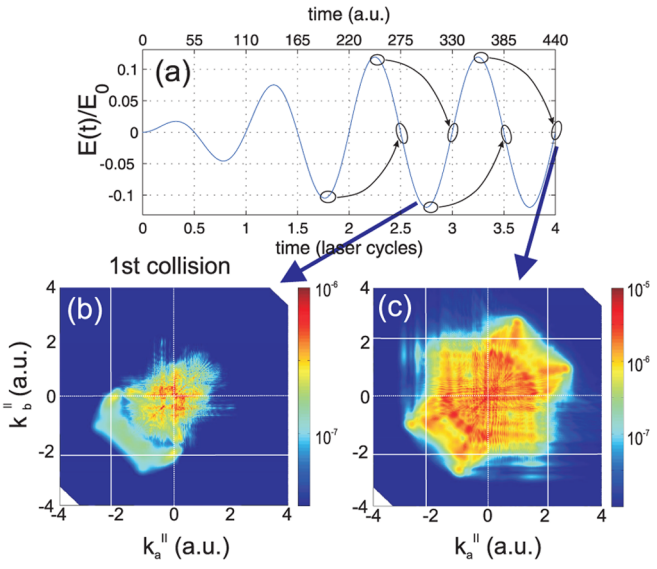

FIG. 2 (color online). Results of an *ab initio* quantum mechanical simulation using a helium model atom interacting with a 4 cycle laser pulse at 800 nm and a peak intensity of 5×10^{14} W/cm^2 (a). Correlated two-electron momentum distribution on a logarithmic scale (b) after the first significant recollision and (c) at the end of the pulse. (Solid lines) $2\sqrt{U_p}$ corresponding to the vector potential at the instant of collision.

partitioning the coordinate space, extracting the double ionization part of the wave function (cf. [18]), taking its Fourier transform, and integrating over the direction perpendicular to the field. Note that these distributions correspond to the canonical momenta $\mathbf{p} = -i\hbar\nabla$ of the two electrons, which correspond in this case to the momentum to be observed outside the field at the detector.

The emission of the two electrons primarily into the same hemisphere as a key signature of a recollision event, as well as a fingerlike structure, are nicely reproduced in the final momentum distribution [Fig. 2(c)]. As in the experimental data, the fingerlike structure extends beyond the limit of $2\sqrt{U_p(t_{\mathrm{rec}})}$ [solid lines in Figs. 2(b) and 2(c)]. Differences in the orientation of the fingerlike structure, as compared to the experimental data, are probably due to the dimensional reduction of the two-electron Hamiltonian in the simulation. The momentum distribution obtained during the pulse [Fig. 2(b)] is due to the first major rescattering event at about $t_{\mathrm{rec}} \approx 275$ a.u. We may note parenthetically that the interferences between the contributions from the different pathways in the final momentum distribution are signatures of the quantum nature of the double ionization process.

As the momentum distribution in the third quadrant [Fig. 2(b)] corresponds mainly to a single rescattering event at $t = 275$ a.u., we are in the position to further analyze it in view of contributions from binary and recoil collisions. To this end we have obtained partial canonical momentum distributions from different spatial configurations of the two electrons. The results are shown in Fig. 3. For the distribution in Fig. 3(a) we have restricted the double ionization coordinate space to electron pairs found in that hemisphere, which corresponds to an emission of both electrons in the direction of the incident electron in the recollision. As discussed above, this emission pattern is a signature of the binary collision scenario. The corresponding momentum distributions confirm that for a binary collision the maximum appears for $k_a^{\parallel} = k_b^{\parallel}$. For the results shown in Fig. 3(b) the coordinate space has been restricted to two electrons leaving the ion into opposite hemispheres. The canonical momentum distribution obtained from this configuration beyond the $2\sqrt{U_p}$ limit has a minimum for both electrons with equal final momentum. Hence, the results of the quantum mechanical simulation strongly support our interpretation that a recoil collision gives rise to the observed fingerlike structure.

Because of the influence of the external field on the emitted electrons the above analysis is imperfect, as can be seen from the fact that contributions in Figs. 3(a) and 3(b) do not fully reconstruct the total momentum distribution in Fig. 2(b). Part of the two-electron continuum wave function, created early in the rescattering event, is redistributed by the field into the hemisphere opposite to the direction of the incident electron (field direction). As can be seen from Fig. 3(c) these contributions provide the

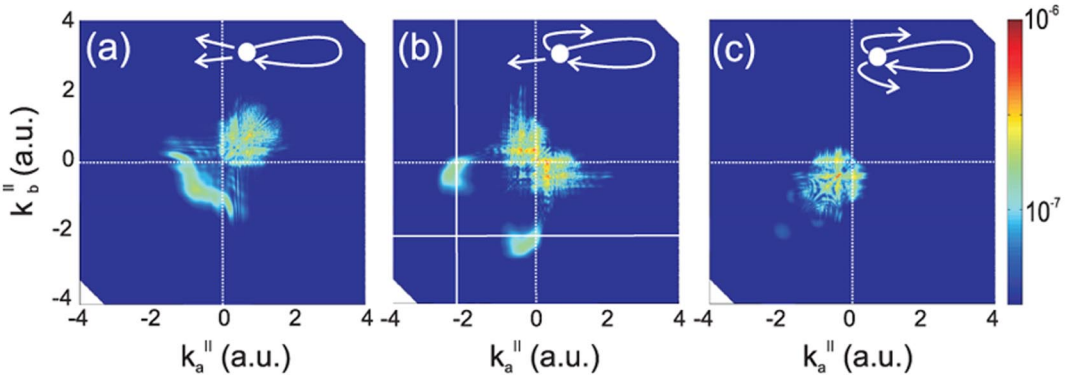

FIG. 3 (color online). Partial two-electron momentum distributions (on logarithmic scale) shortly after the first recollision ($t_{\mathrm{rec}} \approx$ 275 a.u.) for (a) two electrons parallel in the same direction as the incident electron, (b) two electrons in back-to-back direction, and (c) both electrons opposite to the direction of the incident electron. (Solid lines) Maximum drift momentum $2\sqrt{U_p}$.

remaining part of the full momentum distribution. They consist of contributions of both the binary and the recoil recollisions.

In conclusion our experiment on strong field double ionization of helium shows a fingerlike structure in the correlated electron emission. This unveils novel details of the rescattering dynamics establishing a close correspondence between field-free and field-assisted $(e, 2e)$ collision. Classical estimations and *ab initio* results from a fully correlated helium model show that these fingers results from electron-impact ionization with backscattering at the nucleus upon recollision, an analogue to the recoil peak in field-free $(e, 2e)$ collisions.

The experimental work was supported by an NSERC accelerator grant, NSERC Centre of Excellence for Photonic Innovation, NRC HGF science and technology fund, DFG, Alexander von Humboldt Stiftung, and the Studienstiftung des deutschen Volkes.

*andre.staudte@nrc.ca

[1] P. B. Corkum, Phys. Rev. Lett. **71**, 1994 (1993).
[2] T. Rösel, J. Röder, L. Frost, K. Jung, and H. Ehrhardt, J. Phys. B **25**, 3859 (1992).
[3] J. Berakdar, J. Röder, J. S. Briggs, and H. Ehrhardt, J. Phys. B **29**, 6203 (1996).
[4] Th. Weber, H. Giessen, M. Weckenbrock, G. Urbasch, A. Staudte, L. Spielberger, O. Jagutzki, V. Mergel, M. Vollmer, and R. Dörner, Nature (London) **405**, 658 (2000).
[5] B. Feuerstein *et al.*, Phys. Rev. Lett. **87**, 043003 (2001).
[6] E. Eremina, X. Liu, H. Rottke, W. Sandner, A. Dreischuh, F. Lindner, F. Grasbon, G. G. Paulus, H. Walther, R. Moshammer, B. Feuerstein, and J. Ullrich, J. Phys. B **36**, 3269 (2003).
[7] R. Moshammer, J. Ullrich, B. Feuerstein, D. Fischer, A. Dorn, C. D. Schröter, J. R. Crespo López-Urrutia, C. Höhr, H. Rottke, C. Trump, M. Wittmann, G. Korn, K. Hoffmann, and W. Sandner, J. Phys. B **36**, L113 (2003).
[8] E. Eremina, X. Liu, H. Rottke, W. Sandner, M. G. Schätzel, A. Dreischuh, G. G. Paulus, H. Walther, R. Moshammer, and J. Ullrich, Phys. Rev. Lett. **92**, 173001 (2004).
[9] D. Zeidler, A. Staudte, A. B. Bardon, D. M. Villeneuve, R. Dörner, and P. B. Corkum, Phys. Rev. Lett. **95**, 203003 (2005).
[10] J. Chen, J. Liu, L. B. Fu, and W. M. Zheng, Phys. Rev. A **63**, 011404 (2000).
[11] A. Becker and F. H. M. Faisal, Phys. Rev. Lett. **89**, 193003 (2002).
[12] S. L. Haan, L. Breen, A. Karim, and J. H. Eberly, Phys. Rev. Lett. **97**, 103008 (2006).
[13] M. Lein, E. K. U. Gross, and V. Engel, Phys. Rev. Lett. **85**, 4707 (2000).
[14] C. Figueira de Morisson Faria, H. Schomerus, X. Liu, and W. Becker, Phys. Rev. A **69**, 043405 (2004).
[15] J. S. Parker, B. J. S. Doherty, K. T. Taylor, K. D. Schultz, C. I. Blaga, and L. F. DiMauro, Phys. Rev. Lett. **96**, 133001 (2006).
[16] J. S. Prauzner-Bechcicki, K. Sacha, B. Eckhardt, and J. Zakrzewski, Phys. Rev. Lett. **98**, 203002 (2007).
[17] Phay J. Ho, Phys. Rev. A **72**, 045401 (2005).
[18] C. Ruiz, L. Plaja, L. Roso, and A. Becker, Phys. Rev. Lett. **96**, 053001 (2006).
[19] R. Dörner, V. Mergel, O. Jagutzki, L. Spielberger, J. Ullrich, R. Moshammer, and H. Schmidt-Böcking, Phys. Rep. **330**, 95 (2000).
[20] J. Ullrich, R. Moshammer, A. Dorn, R. Dörner, L. Ph. H. Schmidt, and H. Schmidt-Böcking, Rep. Prog. Phys. **66**, 1463 (2003).
[21] A. Alnaser, X. M. Tong, T. Osipov, S. Voss, C. M. Maharjan, B. Shan, Z. Chang, and C. L. Cocke, Phys. Rev. A **70**, 023413 (2004).
[22] N. B. Delone and V. P. Krainov, Phys. Usp. **41**, 469 (1998).
[23] O. Jagutzki, V. Mergel, K. Ullmann-Pfleger, L. Spielberger, U. Spillmann, R. Dörner, and H. Schmidt-Böcking, Nucl. Instrum. Methods Phys. Res., Sect. A **477**, 244 (2002).
[24] T. W. Shyn, Phys. Rev. A **45**, 2951 (1992).